Enhanced Dispersion Resulting from Solute Exchange between Phases

Karen A. Grosser and Kenneth L. Erickson
Fluid and Thermal Sciences Dept., Sandia National Laboratories, Albuquerque, NM 87185

Ruben G. Carbonell
Chemical Engineering Dept., North Carolina State University, Raleigh, NC 27695

The enhanced dispersion resulting from solute exchange between phases was investigated experimentally for the case of a long, cylindrical capillary tube, in which a stationary absorbing phase formed a thin annular film around a flowing fluid. Solute diffusion into the stationary phase was analyzed in detail to accurately determine the coupling of film diffusion and hydrodynamic effects. The experimental results and analyses showed an increase in dispersion relative to the usual Taylor effect. The increased dispersion was a function of the relative partitioning of solute between phases and was in quantitative agreement with predictions from previously published theoretical studies.

Introduction

The combined effect of molecular diffusion and fluid velocity profiles is to induce the solutes in fluids in steady, incompressible, laminar flow to be dispersed relative to the area-averaged fluid velocity. If the flow field is defined well, the hydrodynamic dispersion of solutes resulting from laminar fluid velocity profiles can be estimated *a priori*. Published theoretical analyses have focused on dispersion in long, smooth tubes having relatively simple cross-sections.

Taylor (1953) investigated dispersion of a nonreactive and nonadsorptive solute in a fluid in laminar flow through a long, small-bore tube having circular cross-section. He considered the case where solute transport by molecular diffusion in the axial direction was negligible. Taylor's analysis showed that, with certain restrictions on the physical parameters, dispersion of the solute relative to the area-averaged fluid velocity $\langle v_\alpha \rangle$ could be described by an expression of the form of Fick's law. In his expression, the effective, or Taylor, dispersion coefficient D^* was given by:

$$D^* = \frac{r_1^2 \langle v_\alpha \rangle^2}{48 D_\alpha} \tag{1}$$

where D_α is the molecular diffusion coefficient (assumed constant) for the solute in the fluid, and r_1 is the inside radius of the tube. Taylor also experimentally verified his theoretical predictions. Aris (1956) removed some of the parameter restrictions imposed by Taylor and showed that dispersion of a nonreactive and nonadsorptive solute in a fluid flowing through a tube of arbitrary cross-section depends on the sum of the molecular and Taylor diffusion coefficients for the solute. That is,

$$D^* = D_\alpha + \frac{\Phi b^2 \langle v_\alpha \rangle^2}{D_\alpha} \tag{2}$$

where b is a dimension characteristic of the tube's cross-section, and Φ is a dimensionless constant (determined by the geometry of the cross-section, the fluid velocity profile, and the spatial variation of the molecular diffusion coefficient about its mean value D_α). For a circular cross-section and constant molecular diffusion coefficient, $b = r_1$ and $\Phi = 1/48$, which correspond to Taylor's results. Gill and Sankarasubramanian (1970) further examined dispersion of a nonreactive and nonadsorptive solute in a long tube having circular cross-section and developed a more general solution, valid for all the values of time. Their analysis involved time-dependent dispersion coefficients and for long times converged to the Taylor-Aris result.

Before the works of Taylor and Aris, Westhaver (1942) had investigated analogous dispersion phenomena occurring with

Correspondence concerning this article should be addressed to K. A. Grosser, who was a visiting summer student from the Chemical Engineering Department, North Carolina State University. Her current address: Merck, Sharp, and Dohme Research Laboratories, Rahway, NJ 07065.

a binary mixture in an open-tube distillation column. He considered an ascending laminar flow of vapor and a descending reflux film, which was assumed to evenly wet the tube wall and to have uniform composition in the radial direction. Westhaver further assumed that the average fluid velocity in the descending film was small relative to the ascending vapor velocity and that, in both liquid and vapor phases, transport of the more volatile component or solute by molecular diffusion in the axial direction was negligible. For the total reflux condition, where the fraction of solute retained by the film is unity, Westhaver predicted an effective solute dispersion coefficient similar to that of Taylor, but larger by a factor of 11:

$$D^* = \frac{11 r_1^2 \langle v_\alpha \rangle^2}{48 D_\alpha} \tag{3}$$

Westhaver found good agreement between his predictions and experimental data given by Rose (1936).

The difference between Taylor's and Westhaver's results is due to solute retention by Westhaver's liquid film, which was absent in Taylor's analyses. The general manner in which dispersion is affected by solute exchange with a second phase, uniformly coating the inside of a tube containing a fluid in laminar flow, was examined by Golay (1958) and Aris (1959). Golay analyzed the problem of solute dispersion in a tube with either circular or rectangular (large width to thickness ratio) cross-section. The inner wall of the tube was coated uniformly with a stationary solute-sorbing layer, in which diffusion was assumed to be infinitely fast. The solute was partitioned between phases such that, at equilibrium, the amount of solute in the stationary layer was related to the amount in the flowing fluid by the proportionality constant k, which will be referred to subsequently as the partitioning constant. Golay derived a Fick's law result, in which the effective dispersion coefficient was given by

$$D^* = D_\alpha + \frac{r_1^2 \langle v_\alpha \rangle^2}{48 D_\alpha} \left[\frac{1 + 6k + 11k^2}{(1+k)^2} \right] \tag{4}$$

for tubes having circular cross-section. In the above expression, it can be seen that solute exchange between phase enhances dispersion relative to the case without solute exchange. In particular, the Taylor-Aris dispersion coefficient is increased by a numerical factor that is a function of the relative amount of solute retained by the stationary layer. The value of D^* varies from the Taylor-Aris result, corresponding to $k=0$, to Westhaver's result, corresponding to $k \to \infty$. Golay also provided a limited analysis of the additional dispersion which would result from relatively slow solute diffusion into the stationary layer. Khan (1962) extended Golay's analysis to include an interfacial resistance to mass transfer. Aris (1959) removed the restriction of a stationary solute-sorbing layer and extended his earlier analyses (Aris, 1956) to the case in which a fluid layer uniformly wets the tube's inner wall and flows as an annulus around another flowing fluid with which the annular fluid exchanges solute. The rate of solute exchange was represented by a linear-driving-force expression. The effective dispersion coefficient obtained by Aris was the sum of the Golay-type coefficients for the two phases and a term for the finite rate of solute exchange between the two fluids.

Zanotti and Carbonell (1984) used the method of spatial averaging to develop governing equations for the average concentration of a solute being transferred between two phases moving in one-dimensional axisymmetric flow in a cylindrical tube, in which one phase forms a uniform annulus around the other. The governing equations consisted of two coupled partial differential equations that described the area-averaged solute concentration in each phase and contained terms for solute transport by molecular diffusion and hydrodynamic dispersion. The two-equation model developed by Zanotti and Carbonell provides an accurate description of the effects of relatively slow solute diffusion into a sorbing annular phase and yields a simpler model than that given by Paine et al. (1983) for describing dispersion when irreversible adsorption occurs at the tube wall. Furthermore, for appropriate physical parameter restrictions, the two equations of Zanotti and Carbonell yield results corresponding to those given by Taylor (1953), Aris (1956), Westhaver (1942), Golay (1958), Khan (1962), and Aris (1959).

Quantitative experimental evaluation of the theoretical models predicting dispersion when a solute is exchanged between a flowing fluid and another phase, either stationary or flowing, has been limited. As mentioned above, Taylor (1953) and Westhaver (1942) found good agreement between experimental and theoretical results for the extreme cases of $k=0$ and $k \to \infty$, respectively. For intermediate cases, k having values of about 1 to 10, qualitative experimental evaluation of Golay's results was provided by Desty and Goldup (1960) and Scott and Hazeldean (1960), who examined the effects of operating parameters on the performance of capillary chromatography columns. The trends in column performance that they observed with respect to variations in column diameter, stationary film thickness, gas velocity, partitioning constant, and solute diffusion coefficients in the fluid and in the stationary phase were consistent with Golay's results. However, the experimentally determined numerical constants in the dispersion expressions differed considerably, by as much as a factor of four, from the values calculated from Golay's expression. The reasons for the discrepancies were not fully resolved, due partially to experimental uncertainties and errors in estimating the solute diffusion coefficient in the stationary phase.

The purpose of this work was to provide quantitative experimental evaluation of the theoretically predicted dispersion that results when a solute is exchanged between a flowing fluid and stationary solute-sorbing phase. Specifically, experiments were done using a long, cylindrical capillary with a thin, stationary coating on its inner wall, and the data obtained were used to evaluate a reduced form of the two-equation model given by Zanotti and Carbonell (1984) and, as a direct consequence, the results given by Golay (1958). The analysis of experimental results showed that the observed dispersion was in quantitative agreement with the theoretical predictions. While the simplest geometry is considered here, it is worth noting that the effect that solute exchange between phases has on dispersion is a general phenomenon, which will occur in more practical geometries such as packed beds. In this case, solute exchange may result from diffusion and reaction in the void volume of porous catalysts or from adsorption and absorption by porous and nonporous sorbents. It is, however, much more difficult to predict and experimentally verify the numerical constants in the dispersion expressions for such cases.

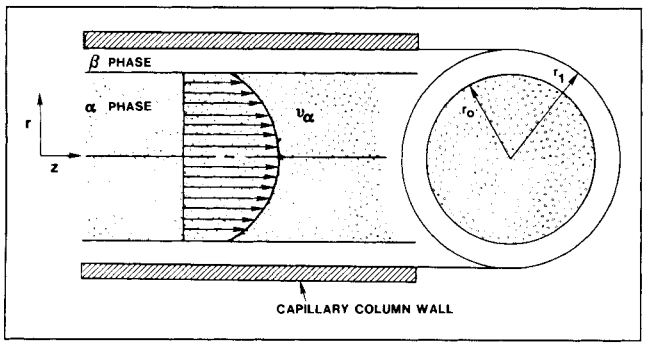

Figure 1. Capillary tube.

Theory

Consider the cylindrical capillary tube shown schematically in Figure 1. The inner wall of the tube forms an inert, impermeable boundary around two phases, α and β, between which a solute is exchanged. The α phase is a moving fluid, and the β phase is a stationary fluid, or a solid, which is bonded to the capillary wall and forms a uniform annulus around the α phase. The length L of the capillary tube is taken to be large relative to the inner radius r_0 of the annular β phase, and the difference between r_0 and the outer radius r_1 is small relative to r_0. The solute material balances for the α and β phases are

$$\frac{\partial c_\alpha}{\partial t}+v_\alpha(r)\frac{\partial c_\alpha}{\partial z}=D_\alpha\frac{\partial^2 c_\alpha}{\partial z^2}+D_\alpha\frac{1}{r}\frac{\partial c_\alpha}{\partial r}\left(r\frac{\partial c_\alpha}{\partial r}\right),\quad 0<r<r_0 \tag{5}$$

and

$$\frac{\partial c_\beta}{\partial t}=D_\beta\frac{\partial^2 c_\beta}{\partial z^2}+D_\beta\frac{1}{r}\frac{\partial c_\beta}{\partial r}\left(r\frac{\partial c_\beta}{\partial r}\right),\quad r_0<r<r_1 \tag{6}$$

where c_α and c_β denote the local solute concentrations in the α and β phases, respectively, and v_α the local velocity of the α phase. These equations are based on one-dimensional, laminar, steady, axisymmetric flow of the α phase in the region $0<r<r_0$, and on the assumption that molecular diffusion of the solute in the α and β phases can be described by Fick's law with constant diffusion coefficients D_α and D_β. In this work, $D_\alpha>>D_\beta$, and the β phase is assumed to be uniformly coated on the capillary wall. At the center and at the wall of the capillary, the solute flux vanishes. At the interface between the α and β phases, it is assumed that there is no interfacial resistance to mass transfer, so that the solute flux is continuous, and local equilibrium exists. Also, it is assumed that solute concentrations are sufficiently dilute so that the equilibrium distribution coefficient K_e for solute exchange between phases is constant.

Two-equation model from volume averaging

As previously noted, Zanotti and Carbonell (1984) applied the method of spatial averaging to the point equations for transport of a solute between two phases that are moving in one-dimensional, axisymmetric flows in a cylindrical geometry. For the case of a long capillary tube in which solute transport is described by Eqs. 5 and 6, the governing equations obtained by Zanotti and Carbonell give the following two-equation model when the α-phase velocity profile is parabolic, and $D_\alpha>>D_\beta$,

$$\frac{\partial\langle C_\alpha\rangle}{\partial t}+\left(1+\frac{\gamma}{12}\right)\langle v_\alpha\rangle\frac{\partial\langle C_\alpha\rangle}{\partial z}=\frac{\gamma}{24}\langle v_\alpha\rangle\frac{\partial\langle C_\beta\rangle}{\partial z}+\left(D_\alpha+\frac{\langle v_\alpha\rangle^2 r_0^2}{48D_\alpha}-\frac{\gamma\langle v_\alpha\rangle^2 r_0^2}{576D_\alpha}\right)\frac{\partial^2\langle C_\alpha\rangle}{\partial z^2}+\frac{\gamma D_\alpha}{r_0^2}(\langle C_\beta\rangle-\langle C_\alpha\rangle) \tag{7}$$

and

$$\frac{\partial\langle C_\beta\rangle}{\partial t}=\frac{\gamma\langle v_\alpha\rangle}{24k}\frac{\partial\langle C_\alpha\rangle}{\partial z}-\frac{\gamma D_\alpha}{r_0^2 k}(\langle C_\beta\rangle-\langle C_\alpha\rangle) \tag{8}$$

where $\langle C_\alpha\rangle$ and $\langle C_\beta\rangle$ are the normalized values of the area-averaged concentrations $\langle c_\alpha\rangle$ and $\langle c_\beta\rangle$, respectively, and are defined by $\langle C_\alpha\rangle=\langle c_\alpha\rangle/c^*$ and $\langle C_\beta\rangle=\langle c_\beta\rangle/K_e c^*$; the reference concentration c^* is defined as $(1/t^*)\int_0^{t^*}\langle c_\alpha(L,t)\rangle dt$, where t^* denotes unit time; the term $\langle v_\alpha\rangle$ is the area-averaged value of v_α;

$$k=\frac{K_e(r_1^2-r_0^2)}{r_0^2} \tag{9}$$

and

$$\gamma=\left[\frac{1}{8}+\frac{(r_1-r_0)^2 D_\alpha}{3kr_0^2 D_\beta}\right]^{-1} \tag{10}$$

The criteria for applying spatial averaging were that

$$\frac{LD_\alpha}{\langle v_\alpha\rangle r_0^2}>>1 \text{ and } \frac{LkD_\beta}{\langle v_\alpha\rangle(r_1-r_0)^2}>>1 \tag{11}$$

As the left side of each inequality becomes increasingly larger, the difference between exact and approximate values becomes very small. Conversely, as the left side decreases below unity, the errors associated with the approximation increase. This was demonstrated analytically by Zanotti and Carbonell (1984) for some simpler cases than considered in this work, and Erickson et al. (1986) reported similar results for the case of dispersion resulting from only film diffusion effects. In the experiments described below,

$$\frac{LD_\alpha}{\langle v_\alpha\rangle r_0^2}\ (O)\ 10^4 \text{ and } \frac{LkD_\beta}{\langle v_\alpha\rangle(r_1-r_0)^2}\ (O)\ 10^2$$

and the two-equation model obtained from spatial averaging should be a good approximation.

During the experiments, significant dispersion occurred in the capillary because of solute exchange between phases; however, at the column inlet and outlet, molecular diffusion and Taylor dispersion were negligible. At the capillary inlet ($z=0$), the corresponding boundary condition is

$$\langle C_\alpha(0,t)\rangle=F(t) \tag{12}$$

where $F(t)$ is a known function. At the outlet ($z=L$), the appropriate boundary condition is

$$\frac{\partial\langle C_\alpha(L,t)\rangle}{\partial z}=0=\frac{\partial\langle C_\beta(L,t)\rangle}{\partial z} \tag{13}$$

and for a very long capillary, the above boundary condition can be replaced by

$$\langle C_\alpha(z\to\infty,t)\rangle=0=\langle C_\beta(z\to\infty,t)\rangle \tag{14}$$

which is more convenient for attempting analytical solutions (Levenspiel, 1962).

The choice of boundary conditions is related to satisfying the previously stated criteria (Eq. 11) for applying spatial averaging. When the criteria are satisfied, the above boundary conditions are valid. If the criteria are not satisfied, then those boundary conditions, as well as the two-equation model, are not applicable. As a practical consideration, when the criteria are satisfied, the effect of the boundary condition is small. For example, tracer responses were calculated using both the condition given by Eq. 13 and the simplified condition given by Eq. 14. The difference between the tracer responses calculated with each boundary condition was negligible.

The two-equation model given by Eqs. 7 and 8 exhibits some unusual coupling terms that do not appear in the equations derived by a shell balance approach (Zanotti and Carbonell, 1984). For selected cases, Zanotti and Carbonell (1984) compared the average concentrations given by the two-equation model with those given by the numerical solution of the point equations and obtained good agreement.

Film diffusion model: negligible dispersion

Equations 5 and 6 can be simplified for the case of negligible dispersion in the capillary. In this case, c_α is essentially independent of radial position, and solute transport by molecular diffusion in the axial direction is negligible. The area average of Eq. 5 then can be written as

$$\frac{\partial\langle C_\alpha\rangle}{\partial t}+\langle v_\alpha\rangle\frac{\partial\langle C_\alpha\rangle}{\partial z}+\frac{2}{r_0}\frac{\partial M}{\partial t}=0 \tag{15}$$

and for the case considered here, where $(r_1-r_0)/r_0<<1$, Eq. 6 becomes

$$\frac{\partial C_\beta}{\partial t}=D_\beta\frac{\partial^2 C_\beta}{\partial r^2} \tag{16}$$

where $C_\beta=c_\beta/c^*K_e$, and M is given by

$$M=K_e\int_{r_0}^{r_1}C_\beta dr \tag{17}$$

Again, the solute flux vanishes at r_1, and equilibrium ($C_\beta=\langle C_\alpha\rangle$) is assumed at the interface $r=r_0$.

As discussed later, the film diffusion model given by Eqs. 15-17 provides a convenient means for evaluating the β-phase solute diffusion coefficient D_β. In this work, the initial solute concentration in both phases is zero, and the α-phase concentration at the capillary inlet is a known function $F(t)$.

The problem, analogous to Eqs. 15-17, of solid diffusion in a fixed bed of uniform spheres was solved by Rosen (1952, 1954) for the case in which $F(t)$ was the unit step function. His analyses were extended to flat plates by Erickson et al. (1984). The solution for a thin annulus follows directly from the flat plate results. For

$$\frac{D_\beta kL}{\langle v_\alpha\rangle(r_1-r_0)^2}>50$$

as in the experiments described below, the effluent solute concentration $\langle C_\alpha(L,t)\rangle$ is given approximately (less than 1% error) by the convolution of $F(t)$ with the impulse response $I(L,t)$ of the capillary

$$\langle C_\alpha(L,t)\rangle=\int_0^t F(\tau)I(L,t-\tau)d\tau \tag{18}$$

The impulse response $I(L,t)$ is the time derivative of the unit-step response and is given by

$$I(L,t)=\frac{\sqrt{3}}{\sqrt{\pi}}\frac{\dfrac{D_\beta}{2(r_1-r_0)^2}}{\left[\dfrac{D_\beta kL}{\langle v_\alpha\rangle(r_1-r_0)^2}\right]^{1/2}}\exp(-\omega^2) \tag{19}$$

where

$$\omega=\frac{3\left[\dfrac{D_\beta}{2(r_1-r_0)^2}\right]\left(t-\dfrac{L}{\langle v_\alpha\rangle}\right)}{\left[3\dfrac{D_\beta kL}{\langle v_\alpha\rangle(r_1-r_0)^2}\right]^{1/2}}-\frac{\left[3\dfrac{D_\beta kL}{\langle v_\alpha\rangle(r_1-r_0)^2}\right]^{1/2}}{2} \tag{20}$$

The diffusion coefficient D_β is then evaluated readily by optimizing the value of D_β to give the best least-squares fit between analytical and experimental values of $\langle C_\alpha(L,t)\rangle$. Equation 18 is based on a constant area-averaged velocity $\langle v_\alpha\rangle$. If a significant pressure drop occurs across the column, $\langle v_\alpha\rangle$ will be a function of z, and Eq. 15 must be replaced by

$$\frac{\partial\langle C_\alpha\rangle}{\partial t}+\langle v_\alpha\rangle\frac{\partial\langle C_\alpha\rangle}{\partial z}+\langle C_\alpha\rangle\frac{\partial\langle v_\alpha\rangle}{\partial z}+\frac{2}{r_0}\frac{\partial M}{\partial t}=0 \tag{21}$$

Furthermore, since $\langle v_\alpha(0)\rangle\neq\langle v_\alpha(L)\rangle$, the boundary condition at the capillary inlet must be modified. For an impulse injection at $z=0$,

$$\langle v_\alpha(0)\rangle\langle c_\alpha(0,t)\rangle=\delta(t)\langle v_\alpha(L)\rangle\int_0^\infty\langle c_\alpha(L,t)\rangle dt$$

or

$$\langle C_\alpha(0,t)\rangle=\frac{\langle v_\alpha(L)\rangle}{\langle v_\alpha(0)\rangle}t^*\delta(t) \tag{22}$$

where t^* denotes unit time, and $\delta(t)$ the unit impulse symbol. By analogy with Rosen's (1952, 1954) development for spheres and Erickson et al.'s modification for flat plates, it can be shown that when Eq. 15 is replaced by Eq. 21 and $\langle C_\alpha(0,t)\rangle$ is given by Eq. 22, the corresponding effluent solute concentration $\langle C_\alpha(L,t)\rangle$ is given by Eq. 18 with $\langle v_\alpha\rangle$ replaced by the average axial velocity $\langle\langle v_\alpha\rangle\rangle$ given by

$$\langle\langle v_\alpha\rangle\rangle = \frac{z}{\int_0^z \frac{z}{\langle v_\alpha\rangle}} = \frac{L(1+k)}{\mu'_{1\alpha}(L) - \mu'_{1\alpha}(0)} \tag{23}$$

where $\mu'_{1\alpha}$ is defined below (Eq. 25) as the absolute first moment of $\langle C_\alpha\rangle$ with respect to time.

Analytical moment analysis

If the solute concentration $F(t)$ at the capillary inlet is a pulse-like function, the mean travel time and variance of the pulse response at the capillary outlet can be examined analytically for the two-equation model and film diffusion model given in the previous two sections. The travel time and variance are obtained from the first three analytical moments of $\langle C_\alpha(L,t)\rangle$ with respect to time, which can be obtained using Laplace transforms, without directly solving the governing equations (for example, see Carbonell, 1980; Valocchi, 1985). At a given value of z, and nth moment of $\langle C_\alpha(z,t)\rangle$ with respect to time is denoted by $m_{n\alpha}$ and defined by

$$m_{n\alpha}(z) = \int_0^\infty \langle C_\alpha(z,t)\rangle t^n dt, \quad n = 0,\ 1,\ 2 \tag{24}$$

The zeroth moment $m_{0\alpha}$ represents the total amount of solute entering the α phase, provided that dispersion is negligible upstream from the capillary inlet and downstream from the outlet. The absolute nth moment is defined as

$$\mu'_{n\alpha}(z) = \frac{m_{n\alpha}(z)}{m_{0\alpha}(z)} \tag{25}$$

The absolute first moment ($n=1$) represents the mean travel time for the pulse. The second central moment $\mu_{2\alpha}$ is defined in terms of the first and second absolute moments

$$\mu_{2\alpha}(z) = \mu'_{2\alpha}(z) - [\mu'_{1\alpha}(z)]^2 \tag{26}$$

and represents the variance of the solute concentration relative to the mean travel time.

Consider the case in which the solute concentrations in both α and β phases are initially zero, and the capillary is sufficiently long so that Eq. 14 applies to the two-equation model. This case approximates conditions in the experiments described below. Let $\mu'_{1\alpha}(0)$ and $\mu_{2\alpha}(0)$ denote the absolute first and second central moments of $F(t)$. Then, at $z=L$, the absolute first moment $\mu'_{1\alpha}(L)$ for both the two-equation model (Eqs. 7 and 8) and the film diffusion model (Eqs. 15-17) is given by

$$\mu'_{1\alpha}(L) = \mu'_{1\alpha}(0) + \frac{(1+k)L}{\langle v_\alpha\rangle} \tag{27}$$

The second central moment $\mu_{2\alpha}(L)$ for the two-equation model is given by

$$\mu_{2\alpha}(L) = \mu_{2\alpha}(0) + \frac{Lk}{\langle v_\alpha\rangle}\left[\frac{2(r_1-r_0)^2}{3D_\beta}\right] + \frac{2L(1+k)^2}{\langle v_\alpha\rangle^3}D_\alpha + \frac{2L(1+k)^2}{\langle v_\alpha\rangle^3}D_\alpha\left\{\frac{r_0^2\langle v_\alpha\rangle^2}{48D_\alpha^2}\left[\frac{1+6k+11k^2}{(1+k)^2}\right]\right\} \tag{28}$$

and for the film diffusion model

$$\mu_{2\alpha}(L) = \mu_{2\alpha}(0) + \frac{Lk}{\langle v_\alpha\rangle}\left[\frac{2(r_1-r_0)^2}{3D_\beta}\right] \tag{29}$$

On the right side of Eq. 28, the three terms that are added to $\mu_{2\alpha}(0)$ reflect three separate mechanisms contributing to spreading of the pulse. From left to right, the terms represent film diffusion or solute exchange with the β phase, molecular diffusion in the α phase, and hydrodynamic dispersion in the α phase. It should be noted that the same three terms were obtained by Golay (1958) and Khan (1962) using different approaches.

The dispersion coefficient D^* is related to $\mu_{2\alpha}(L)$ by

$$\mu_{2\alpha}(L) = \mu_{2\alpha}(0) + \frac{Lk}{\langle v_\alpha\rangle}\left[\frac{2(r_1-r_0)^2}{3D_\beta}\right] + \frac{2L(1+k)^2}{\langle v_\alpha\rangle^3}D^* \tag{30}$$

When the capillary wall is inert ($k=0$), the film diffusion term in Eq. 28 is zero, and the molecular diffusion and hydrodynamic dispersion terms give the dispersion coefficient corresponding to the Taylor-Aris result

$$D^* = D_\alpha\left(1 + \frac{r_0^2\langle v_\alpha\rangle^2}{48D_\alpha^2}\right) \tag{31}$$

With reversible adsorption at the capillary wall, the film diffusion term is again zero, but the dispersion coefficient corresponding to Golay's expression is obtained

$$D^* = D_\alpha\left\{1 + \frac{r_0^2\langle v_\alpha\rangle^2}{48D_\alpha^2}\left[\frac{1+6k+11k^2}{(1+k)^2}\right]\right\} \tag{32}$$

The effect that solute partitioning between the α and β phases has on hydrodynamic dispersion can be illustrated by examining the ratio of the dispersion coefficients that are defined by Eqs. 31 and 32 and are denoted by D^*(Taylor) and D^*(Golay), respectively. The ratio D^*(Golay)/D^*(Taylor) is shown in Figure 2, where values are given as a function of the partitioning constant k, with $\langle v_\alpha\rangle$ as a parameter. Figure 2 is based on values of $r_0 = 2.65\times10^{-4}$ m and $D_\alpha = 1.0\times10^{-5}$ m^2/s, which are representative of the experiments discussed

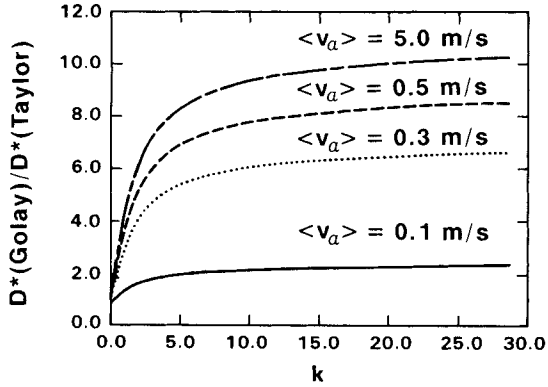

Figure 2. Ratio D^*(Golay)/D^*(Taylor) as a function of k: $D_\alpha = 1.0\times10^{-5}$ m^2/s.

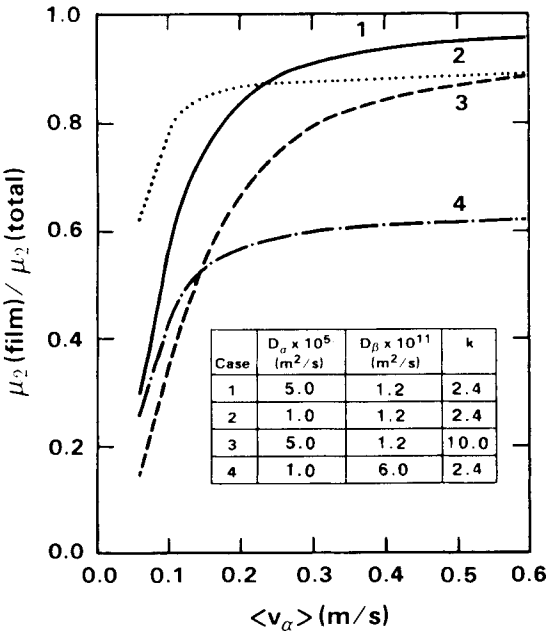

Figure 3. Ratio μ_2(film)/μ_2(total) as a function of $\langle v_\alpha \rangle$.

later. For each value of $\langle v_\alpha \rangle$, the ratio D^*(Golay)/D^*(Taylor) has a different asymptote. For large $\langle v_\alpha \rangle$, the molecular diffusion term is small relative to the hydrodynamic dispersion term, and the ratio is given by

$$\frac{D^*(\text{Golay})}{D^*(\text{Taylor})} \approx \frac{1+6k+11k^2}{(1+k)^2} \tag{33}$$

which has an asymptote of 11, reflecting the previous work of Westhaver (1942). The magnitude of the hydrodynamic term relative to the molecular diffusion term decreases as $\langle v_\alpha \rangle^2$, which results in the decreasing asymptotes shown for the ratio D^*(Golay)/D^*(Taylor).

The effects that the various parameters have on the dispersion and film (β-phase) diffusion terms and the relative amounts that these mechanisms contribute to pulse spreading can be illustrated by examining the ratio μ_2(film)/μ_2(total), where μ_2(film) denotes the difference between $\mu_{2\alpha}(L)$ and $\mu_{2\alpha}(0)$ from Eq. 29, and μ_2(total) the difference from Eq. 28. For several combinations of parameter values, representative of those for this work, the ratio μ_2(film)/μ_2(total) is shown as a function of $\langle v_\alpha \rangle$ in Figure 3. In cases 1 and 3, $D_\alpha = 5.0\times10^{-5}$ m^2/s, $D_\beta = 1.2\times10^{-11}$ m^2/s, and k is 2.4 and 10.0, respectively. In cases 2 and 4, $D_\alpha = 1.0\times10^{-5}$ m^2/s, D_β is 1.2×10^{-11} or 6.0×10^{-11} m^2/s, and $k = 2.4$. In all cases, $L = 30$ m, the film thickness $(r_1 - r_0)$ is 1.2×10^{-6} m and $r_0 = 2.65\times10^{-4}$ m. For each combination of D_α, D_β, and k, the figure shows that the ratio approaches an asymptote as $\langle v_\alpha \rangle$ increases. This occurs because the molecular diffusion term becomes negligible relative to the film diffusion and hydrodynamic terms, which both vary as $1/\langle v_\alpha \rangle$ rather than as $1/\langle v_\alpha \rangle^3$. Figure 3 also shows that for larger $\langle v_\alpha \rangle$, a decrease in D_α or an increase in D_β causes a decrease in μ_2(film)/μ_2(total), because the hydrodynamic term increases relative to the film diffusion term. Conversely, as $\langle v_\alpha \rangle$ becomes small, the molecular diffusion term dominates, and μ_2(film)/μ_2(total) becomes small.

As a final illustration, Figure 4 shows the ratio of the hydrodynamic term in Eq. 28, denoted by μ_2(hydro), to the molecular diffusion term, denoted by μ_2(diff), as a function of $\langle v_\alpha \rangle$, with D_α as a parameter. In cases 1-4, the value of D_α is 1.0×10^{-5}, 2.0×10^{-5}, 3.0×10^{-5} and 5.0×10^{-5} m^2/s, respectively. In all cases, the values for L, film thickness $(r_1 - r_0)$, and r_0 are the same as for Figure 3; the value of D_β is 1.2×10^{-11} m^2/s, and the value of k is 2.4. It can be seen that for $\langle v_\alpha \rangle > 0.12$ m/s and $D_\alpha < 1.0\times10^{-5}$ m^2/s, dispersion is dominated by hydrodynamic effects rather than molecular diffusion.

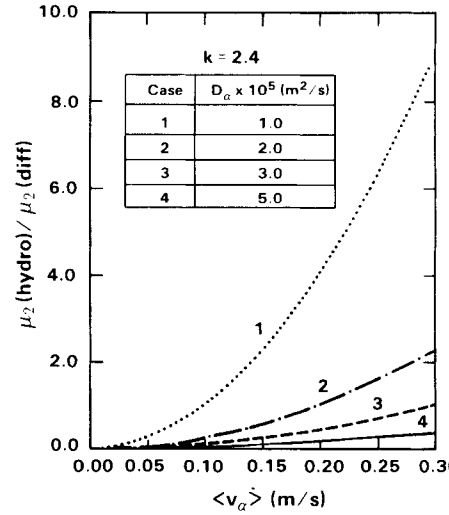

Figure 4. Ratio μ_2(hydro)/μ_2(diff) as a function of $\langle v_\alpha \rangle$.

Experimental Studies

Dispersion data in a long cylindrical capillary tube were obtained using a gas chromatograph (Hach Carle Series 400 AGC, Hach Company, Loveland, CO) fitted with an open-tube capillary column of bonded, fused silica (superox polyethylene glycol, Alltech Associates, Inc., Deerfield, IL). In this case, the α phase was the carrier gas helium, and the β phase was a stationary 1.2-μm-thick film of polyethylene glycol 20M, having a molecular weight of about 20,000. The inside diameter of the capillary was 0.53 mm. Solute gases or vapors were injected into the helium carrier using the chromatograph's eight-port sampling valve. Only trace amounts were injected, since it was necessary to perform experiments with solute concentrations that were small enough so that the absorption equilibrium distribution coefficient K_e and, therefore, the partitioning constant k, as well as the diffusion coefficients D_α and D_β were independent of solute concentration. The values of D_α were calculated from the Chapman-Enskog equation (Reid et al., 1977); however, the values of k and D_β had to be obtained experimentally.

First, a variety of gases and vapors were tested to identify those having k and D_β values that would permit quantitative comparison between predicted and observed dispersion. These experiments, which are subsequently referred to as low-pressure experiments, were done with average column pressures near atmospheric and average gas velocities of about 0.4 m/s. It was assumed, and then verified *a posteriori*, that the molecular diffusion and hydrodynamic dispersion terms in Eq. 28 were small relative to the β-phase diffusion term.

A second set of experiments, which are subsequently referred to as high-pressure experiments, was done with average column

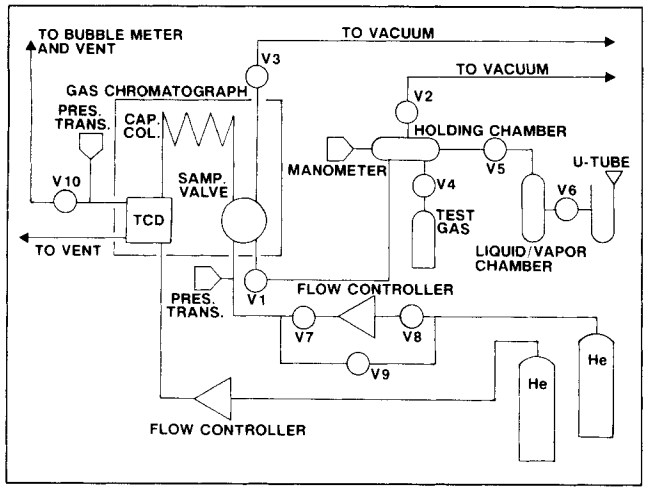

Figure 5. Experimental equipment.

pressures of about 453 kPa (66 psia) and average gas velocities of about 0.1 to 0.3 m/s. In these experiments, the magnitude of the molecular diffusion and hydrodynamic dispersion terms in Eq. 28 were about 15 to 23% of the magnitude of the β-phase diffusion term. The relative increase, due to hydrodynamic dispersion, results from D_α being inversely proportional to pressure (Reid et al., 1977), which causes a relative increase in the hydrodynamic term in Eq. 28.

The differences in the relative effects of the dispersion mechanisms in the low- and high-pressure experiments can be seen in Figure 3. Based on the calculated values of D_α given later, case 1 corresponds to the low-pressure experiments. For $\langle v_\alpha \rangle \geq 0.4$ m/s, the magnitude of the molecular diffusion and hydrodynamic dispersion terms are about 5% (or less) of the magnitude of the β-phase diffusion term. Case 2 corresponds to the high-pressure experiments. For $0.1 \leq \langle v_\alpha \rangle \leq 0.3$ m/s, the molecular diffusion and hydrodynamic dispersion terms are about 15 to 23% of the β-phase diffusion term. Furthermore, case 2 in Figure 3 corresponds to the same parameter values as case 1 in Figure 4, which indicates that for $\langle v_\alpha \rangle > 0.1$ m/s, the ratio μ_2(hydro)/μ_2(diff) is 1 or greater. Therefore, in the high-pressure experiments, the dispersion contribution to μ_2(total) is due primarily to hydrodynamic effects, rather than molecular diffusion in the α phase.

Both the low- and high-pressure experiments were done using the equipment shown schematically in Figure 5. In both cases, argon was used as a standard nonabsorbing tracer. Argon samples, or "blanks," were run using exactly the same experimental conditions as were used for each of the sorbing gases or vapors.

Low-pressure experiments

Procedures for the low-pressure experiments were as follows. First, with valves V7 and V8 open and valve V9 closed, a helium flow rate corresponding to an average carrier gas velocity of 0.4 m/s through the capillary was established by the mass flow controller (Type 825 controller with Type 1511 digital flowmeter readout, Datametrics-Dresser Industries, Inc., Wilmington, ME). The carrier flow rate was then checked using the bubblemeter downstream from valve V10. The carrier gas pressure entering and leaving the chromatograph was monitored by separate absolute pressure transducers (model AP10-54 transducers with Model CD223 digital transducer indicator, Validyne Engineering Corporation, Northridge, CA). Preliminary measurements [using a 0.1-m length of 1/8-in. (3.2-mm) stainless steel tubing] showed that for the gas velocities used, the pressure drop through the connecting plumbing between the transducers was negligible relative to the pressure drop through the capillary after it was connected to the plumbing. The helium flow to the reference side of the thermal conductivity detector (TCD) also was maintained by a mass flow controller (Type 825).

To test a gas or vapor for appropriate values of k and D_β, valves V1, V2, and V3 were opened, and the holding chamber, sampling valve, and connecting plumbing were evacuated to less than 1.3 Pa (0.01 torr), after which the valves were closed. Bottled gases were then admitted to the holding chamber through valve V4, and vapors from the liquid/vapor chamber were admitted through valve V5. Both gases and vapors were admitted to the holding chamber until the desired chamber pressure, about 0.13 to 1.3 kPa (1 to 10 torr), was obtained. Valve V1 then was opened, after closing valves V2, V3, V4, and V5. The sample loop (0.25 mL) and associated plumbing were filled with gas or vapor at the pressure in the holding chamber, the volume of which was much greater than that of the sample loop and plumbing. The liquid/vapor chamber contained a small amount of liquid in equilibrium with its vapor. To add liquid to the chamber, valves V2 and V5 were opened and the holding chamber, liquid/vapor chamber, and associated plumbing were evacuated to less than 1.3 Pa (0.01 torr). With valves V2 and V5 closed, the U-tube was filled with liquid. Keeping the U-tube full, valve V6 was opened, and a small amount of liquid admitted to the chamber.

The experiments were initiated by functioning the sampling valve and injecting the tracer gas or vapor into the carrier gas flowing through the capillary. The tracer response from the TCD was recorded on a chart recorder and subsequently digitized for analysis. Duplicate experiments were done for each gas or vapor, including argon and yielded essentially identical results. Temperatures were 298 ± 1 K. The average column pressure was about 97 kPa (14.2 psia), and the pressure drop across the capillary tube was about 28 kPa (4 psi).

To determine if the partitioning constant k was independent of tracer concentration, the pressure of each of the gases or vapors admitted to the 0.25-mL sample loop was varied by an order of magnitude. The same absolute first moments for the vapor concentration at $z = L$ were obtained, which indicated that the partitioning constant k for each vapor was a constant at the concentrations used.

A similar technique using polymer-coated capillary columns was employed by Pawlish et al. (1986) to obtain diffusion coefficients for various solutes in polystyrene. The diffusion coefficients that they measured agreed well with literature data that were obtained by traditional vapor sorption experiments, in which a sample of known mass is exposed to a constant concentration of penetrant, and the mass gained by the sample is measured as a function of time.

High-pressure experiments

Procedures for the high-pressure experiments were similar to those for the low-pressure experiments. The principal exception was that the carrier flow rate to the sampling valve was established by bypassing the flow controller and adjusting

the regulator pressure, the chromatograph carrier control valve, and a needle valve downstream from the TCD. The regulator and valves were adjusted until the capillary outlet pressure was stable at about 453 kPa (66 psia), and the flow rate, determined with the bubblemeter, was stable and corresponded to gas velocities of about 0.1 to 0.3 m/s in the capillary. Duplicate experiments were done for each gas or vapor, including argon, and yielded essentially identical results. The temperature was 298 ± 1 K. The pressure drop across the capillary was about 7 to 28 kPa (1 to 4 psi). Again, to verify that the partitioning constant k was constant, the pressure of each gas or vapor admitted to the 0.25-mL sample loop was varied by an order of magnitude. Again, no variation in absolute first moments was observed.

Analysis

Analysis of the experimental data first required evaluation of some potentially important variations between theoretical and experimental conditions. In particular, the previously summarized theory was based on a straight, uniformly-coated capillary, and equations were derived in terms of the area-average solute concentration. The experiments, however, employed a coiled capillary, in which the coating could not be examined in complete detail, and the average solute concentration determined by the thermal conductivity detector was probably closest to the flow average. The potential impact that these variations could have on the experimental results are discussed below and are shown to be small. The procedures for analyzing the experimental data are then summarized.

Effect of coiling

In the high-pressure experiments to examine the effects of hydrodynamic dispersion, the ranges of values for the Reynolds, Schmidt, and Dean numbers, and the curvature ratio were, respectively.

$$N_{Re} = \frac{2r_0 \langle \langle v_\alpha \rangle \rangle \rho}{\mu} = 2.5 \text{ to } 4.3 \tag{34}$$

$$N_{Sc} = \frac{\mu}{\rho D_\alpha} = 2.9 \text{ to } 3.2 \tag{35}$$

$$N_{De} = N_{Re}\sqrt{\frac{2r_0}{d_c}} = 0.13 \text{ to } 0.23 \tag{36}$$

$$\lambda = \frac{d_c}{2r_0} = 358 \tag{37}$$

where d_c is the coil diameter of the capillary tube; μ, the carrier gas viscosity; and ρ, the carrier gas density. For N_{Re}, N_{Sc}, and N_{De} in the above ranges of values and for a curvature ratio of 358, the experimental studies reported by Van Andel et al. (1964) and by Trivedi and Vasudeva (1975) indicate that coiling of the capillary would negligibly effect solute dispersion. Similarly, the theoretical work of Nunge et al. (1972), Dean (1928), and Kalb and Seader (1974) indicate negligible effects of coiling the capillary.

Area-average vs. flow-average concentration

The average concentration given by the thermal conductivity detector is probably closest to the flow average. However, for the conditions used in our experiments, the difference between the area-averaged concentration $\langle c_\alpha \rangle$ and the flow-averaged concentration $\overline{c_\alpha}$ is small, which can be shown as follows. Let

$$c_\alpha(r,z,t) = \langle c_\alpha(z,t) \rangle + \tilde{c}_\alpha(r,z,t) \tag{38}$$

where $\tilde{c}_\alpha$ is a fluctuation about the average $\langle c_\alpha \rangle$. The basic assumption for applying spatial averaging is that $|\tilde{c}_\alpha| / \langle c_\alpha \rangle << 1$, which is valid when the inequality given in Eq. 11 is satisfied. To compare area- and flow-averaged concentrations, consider a reasonable concentration profile, such as the parabolic one given by

$$c_\alpha(r,z,t) = c_\alpha(r_0,z,t) + \left[1 - \left(\frac{r}{r_0}\right)^2\right] \Delta c \tag{39}$$

where

$$\Delta c = c_\alpha(r_0,z,t) - c_\alpha(0,z,t) \tag{40}$$

Then

$$\langle c_\alpha \rangle = \frac{2}{r_0^2}\int_0^{r_0} c_\alpha r dr = c_\alpha(r_0,z,t) + \frac{\Delta c}{2} \tag{41}$$

and

$$\tilde{c}_\alpha = \left[\frac{1}{2} - \left(\frac{r}{r_0}\right)^2\right] \Delta c \tag{42}$$

The flow-averaged concentration $\overline{c_\alpha}$ is given by

$$\overline{c_\alpha} = \frac{\frac{2}{r_0^2}\int_0^{r_0} v_\alpha c_\alpha r dr}{\frac{2}{r_0^2}\int_0^{r_0} v_\alpha r dr} \tag{43}$$

and for the parabolic velocity profile given by

$$v_\alpha = 2\langle v_\alpha \rangle \left[1 - \left(\frac{r}{r_0}\right)^2\right] \tag{44}$$

the resulting expression for $\overline{c_\alpha}$ is

$$\overline{c_\alpha} = \langle c_\alpha \rangle + \frac{\Delta c}{6} \tag{45}$$

A reasonable upper bound for Δc is about $0.2\langle c_\alpha \rangle$, in which case $\overline{c_\alpha} \approx 1.03\langle c_\alpha \rangle$. Thus, the difference between area- and flow-averaged concentrations is small.

Film uniformity

The average film thickness that is specified by the manufacturer (Alltech) is determined by using the amount of coating material that is needed to produce a uniform annular coating in a capillary of given length and diameter. The basic techniques for coating capillary columns are well established and widely employed, as discussed by Bolvari et al. (1989). The manufacturer Alltech has prepared polyethyleneglycol-coated columns for several years and maintained excellent reproducibility in column performance.

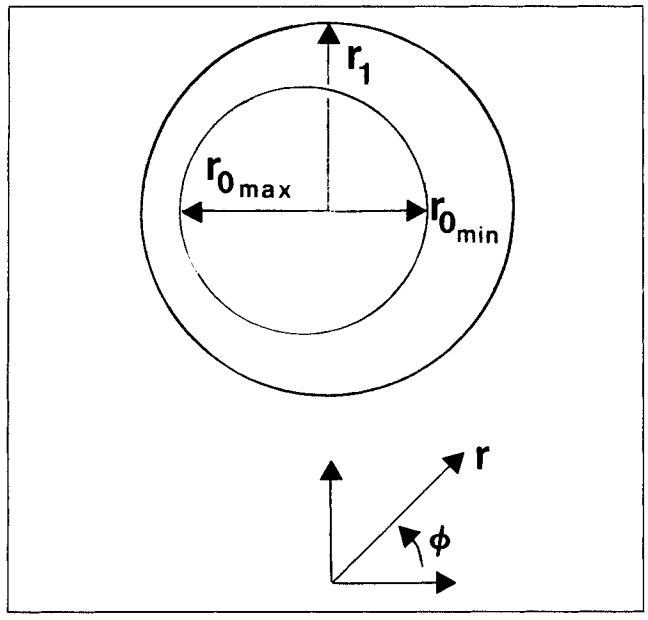

Figure 6. Film asymmetry.

Laurence and coworkers (Pawlisch et al., 1987, 1988; Arnold and Laurence, 1989) have extensively used coated capillary columns to determine solute diffusion coefficients in polymers. The issue of coating uniformity was examined in detail by Pawlisch et al. (1987, 1988). Their columns were coated using techniques similar to those described by Bolvari et al. Several columns were sectioned, and the axial uniformity of the average film thickness examined. The average thickness and average interior diameter were determined indirectly by measuring the column mass, coating mass, and outside column diameter. The variability in coating thickness was less than $\pm 1.25\%$, and indicated that the axial distribution of the coating material was very uniform. The uniformity of their coatings was further evaluated by examining several samples, from each sectioned column, in the scanning electron microscope. Micrographs of cross-sections taken at several points along the length of each column showed the coating to be a smooth, continuous (completely covering the column wall) annular film having a high degree of axial uniformity and good adhesion to the column wall. In a few columns, the coating exhibited a small eccentricity, in which the azimuthal variations in coating thickness occurred smoothly and gradually. Figure 6 illustrates the nature of the observed asymmetry. The ratio, $r_{0_{min}}/r_{0_{max}}$, of the minimum of r_0 to the maximum value, was 0.6 or greater for all of the asymmetric samples.

It was also noted by Pawlisch et al. (1987) that the macroscopic uniformity of the film can be examined visually and that any significant film irregularity acts as a lens for light passing through the column and is readily apparent. Prior to initiating experiments, the Alltech column was visually examined and no irregularities were detected (which indicated a smooth continuous film, rather than a globular one). After completing the low- and high-pressure experiments, the column was reinspected to include examination of randomly selected regions (about 30-cm-long) with a stereoscopic microscope. Again, no macroscopic flaws were observed.

While the coating was certainly not absolutely uniform, there is ample reason given above to believe that variations in coating thickness were negligible, particularly with respect to axial uniformity. If any significant nonuniformities were present, they would have been relatively small, smooth, continuous variations in the azimuthal rather than axial direction.

The net effect of such azimuthal variations is an increase in solute dispersion relative to that for the same conditions with an azimuthally-uniform film. However, in the experiments described previously, the additional dispersion is small and compensated for when an effective film-phase solute diffusion coefficient is evaluated from the experimental data. This can be shown as follows.

If the average film thickness is small relative to the capillary diameter, then variations in $r_0(\phi)$ can be neglected. Furthermore, if the azimuthal variation in film thickness, $r_1 - r_0(\phi)$, is gradual and of the order observed by Pawlisch et al. (1988), then solute diffusion in the film would occur primarily in the radial direction and could be neglected in the aximuthal and axial directions. In the low-pressure experiments, molecular diffusion and hydrodynamic dispersion in the capillary were negligible. In the case of an azimuthally-varying film thickness, the equations analogous to Eqs. 15–17 are:

$$\frac{\partial \langle C_\alpha \rangle}{\partial t} + \langle v_\alpha \rangle \frac{\partial \langle C_\alpha \rangle}{\partial z} + \frac{2}{\bar{r}_0} \frac{\partial M_\phi}{\partial t} = 0 \tag{46}$$

$$\frac{\partial C_\beta}{\partial t} = D_\beta \frac{\partial^2 C_\beta}{\partial r^2} \tag{47}$$

$$M_\phi(z,t) = \frac{K_e}{2\pi} \int_0^{2\pi} \int_{r_{0(\phi)}}^{r_1} C_\beta(r,\phi,z,t)\, dr d\phi \tag{48}$$

Let

$$r_1 - r_0(\phi) = (r_1 - \bar{r}_0) - \epsilon(\phi) = (r_1 - \bar{r}_0)\left[1 - \frac{\epsilon(\phi)}{r_1 - \bar{r}_0}\right] \tag{49}$$

where

$$\bar{r}_0 = \frac{1}{2\pi} \int_0^{2\pi} r_0(\phi)\, d\phi \tag{50}$$

The solution to Eqs. 46–48 is analogous to that for Eqs. 15–17. For

$$\frac{D_\beta k L}{\langle v_\alpha \rangle (r_1 - \bar{r}_0)^2} > 50 \tag{51}$$

as in the low-pressure experiments, the solution to Eqs. 46–48 is given by Eq. 18, where the impulse response $I_\phi(L,t)$ of the capillary is given by

$$I_\phi(L,t) = \frac{\sqrt{3}}{\sqrt{\pi}} \frac{\dfrac{(D_\beta/g)}{2(r_1 - \bar{r}_0)^2}}{\left[\dfrac{(D_\beta/g)kL}{\langle v_\alpha \rangle (r_1 - \bar{r}_0)^2}\right]^{1/2}} \exp(-\omega_\phi^2) \tag{52}$$

where

$$\omega_\phi = \frac{3\left[\frac{(D_\beta/g)}{2(r_1-\bar{r}_0)^2}\right]\left(t-\frac{L}{\langle v_\alpha\rangle}\right)}{\left[3\frac{(D_\beta/g)kL}{\langle v_\alpha\rangle(r_1-\bar{r}_0)^2}\right]^{1/2}} - \frac{\left[3\frac{(D_\beta/g)kL}{\langle v_\alpha\rangle(r_1-\bar{r}_0)^2}\right]^{1/2}}{2} \tag{53}$$

$$g = \frac{1}{2\pi}\int_0^{2\pi}\left[1-\frac{\epsilon(\phi)}{r_1-\bar{r}_0}\right]^3 d\phi \tag{54}$$

and

$$k = \frac{2(r_1-\bar{r}_0)K_e}{\bar{r}_0}$$

Equation 52 is Eq. 19 with D_β replaced by the effective diffusion coefficient, $D_e = D_\beta/g$, and r_0 by $\bar{r}_0$.

Thus, the net effect of an azimuthal variation in film thickness is an increase in dispersion relative to the case of an uniform film. This increase corresponds to an effective decrease in the film-phase solute diffusion coefficient. Let

$$\ell = 1-\frac{\epsilon(\phi)}{r_1-\bar{r}_0} \tag{55}$$

A reasonable expression for ℓ is

$$\ell(\phi) = \ell_1 + (\ell_2-\ell_1)\frac{\phi}{\pi}$$

where ℓ_1 and ℓ_2 are the minimum and maximum values of ℓ, respectively. The resulting expression for g is

$$g = \frac{1}{4}\left(\frac{\ell_2^4-\ell_1^4}{\ell_1-\ell_2}\right) \tag{56}$$

For $r_{0_{min}}/r_{0_{max}} \geq 0.6$ (as observed by Pawlisch et al.), the corresponding bounds on the values of ℓ_1 and ℓ_2 are $0.75 \leq \ell_1 \leq 1.0$ and $1.0 \leq \ell_2 \leq 1.25$, respectively. From which, the range of values for g is $1.0 \leq g \leq 1.06$, which represents a maximum error of 6% in the value of D_β obtained from the low-pressure experiments.

The objective of this work was to examine hydrodynamic dispersion. This was done with the high-pressure experiments. The values of D_β obtained from the low-pressure experiments were used to calculate the film-diffusion contribution to the total dispersion measured in the high-pressure experiments to evaluate the hydrodynamic contribution. Regardless of whether the coating was uniform or azimuthally varying, the diffusion coefficient from the low-pressure experiments yields the correct film-phase dispersion contribution (assuming that the contributions from each dispersion mechanism are additive, as discussed by Aris, 1959) and is appropriate for evaluating hydrodynamic effects.

In the high-pressure experiments, the remaining issue is the effect which possible film asymmetries could have on hydrodynamic dispersion. Since dispersion resulting from film diffusion and hydrodynamic effects are both governed by solute diffusion in the radial direction, perpendicular to the direction of fluid flow, the relative effect of any asymmetries on hydrodynamic dispersion should be on the same order as on dispersion from film diffusion. In the high-pressure experiments, hydrodynamic effects were substantially less than film diffusion effects, and relative errors on the order of 6% in the hydrodynamic effects are near the limits of experimental resolution.

Parameter evaluation and dispersion analysis

In the low-pressure experiments, the pressure drop across the column was large enough so that the average axial velocity $\langle\langle v_\alpha\rangle\rangle$ given by Eq. 23 had to be used in the analysis of data. For consistency and accuracy, $\langle\langle v_\alpha\rangle\rangle$ was also used in the analysis of data from the high-pressure experiments, even though $\langle v_\alpha\rangle$ was approximately constant.

In both the low- and high-pressure experiments, the partitioning constant k for the absorbing vapors, either ethanol or 1-propanol, was evaluated by inspection of the difference between the absolute first moments for the absorbing vapor and the nonabsorbing gas argon. Let $\mu'_{1\alpha k}$ denote the moment for ethanol or 1-propanol ($k>0$), and $\mu'_{1\alpha 0}$ the moment for argon ($k=0$) at the same experimental conditions. For argon, dispersion in the capillary column was negligible in both the low-pressure and high-pressure experiments. Thus, the argon response $\langle C_\alpha(L,t)\rangle$ corresponded to the argon input function $\langle C_\alpha(0,t)\rangle$ translated with respect to time. The input function was obtained from $\langle C_\alpha(L,t)\rangle$ by transforming the values of t so that the first measurable argon concentration at $z=0$ occurred at $t=\Delta t$, where Δt was the time increment used in numerical calculations. It was assumed that for the same experimental conditions, $\langle C_\alpha(0,t)\rangle$ would be the same for argon, ethanol, and 1-propanol. Therefore, $\mu'_{1\alpha k}(0) = \mu'_{1\alpha 0}(0)$, and

$$k = \left[\frac{\mu'_{1\alpha k}(L)-\mu'_{1\alpha 0}(0)}{\mu'_{1\alpha 0}(L)-\mu'_{1\alpha 0}(0)}\right] - 1.0 \tag{57}$$

The molecular diffusion coefficients D_β for ethanol and 1-propanol in the β phase were evaluated by optimizing the value of D_β to give the best least squares fit between the experimental values of $\langle C_\alpha(L,t)\rangle$ from the low-pressure experiments and the corresponding analytical values given by Eq. 18. This procedure was necessary because of ambiguity in comparing the experimental data with the analytical moment expressions. In particular, the baseline drift in the detector response made the use of second central moments difficult, since there was uncertainty in deciding where the pulse ended and the baseline drift began. The optimization was done using a Gauss-Levenberg method (IMSL, 1980). The small amount of dispersion, about 5%, in these experiments was neglected, since it was of the same order as possible experimental uncertainties.

To evaluate the two-equation model, Eqs. 7 and 8 were solved numerically, again because there was ambiguity in comparing the experimental data with the analytical moment expressions. The solution of the two-equation model given by Eqs. 7 and 8 was accomplished using an ordinary differential equation solver (Shampine, 1980) to determine the solute concentration profiles at each time step. It was convenient to solve the equations using the dimensionless axial coordinate $Z = zD_\alpha/\langle\langle v_\alpha\rangle\rangle r_0^2$. Central differencing was performed on all terms except for the convective terms. The convective terms caused some difficulties in solving the equations, since the cell Peclet number ($\Delta Z\langle\langle v_\alpha\rangle\rangle/D_\alpha$) was greater than 20 using 1,000 grid

Table 1. Values of k and D_β

Vapor	$\langle\langle v_\alpha\rangle\rangle$ (m/s)	k	D_β (m²/s)
Ethanol	0.413	2.4	1.2×10^{-11}
1-Propanol	0.419	5.3	8.7×10^{-12}

points over the column length. The difficulties were overcome by using second-order up-winding (Leonard, 1979) on the convective terms. For example, the derivative $\partial\langle C_\alpha\rangle/\partial Z$ was differenced as follows:

$$\frac{\partial\langle C_\alpha\rangle}{\partial Z}=\frac{(\langle C_\alpha\rangle^{i+1}-\langle C_\alpha\rangle^{i-1})}{2\Delta Z}-\frac{\langle C_\alpha\rangle^{i+1}}{8\Delta Z}+\frac{3\langle C_\alpha\rangle^{i}}{8\Delta Z}-\frac{3\langle C_\alpha\rangle^{i-1}}{8\Delta Z}+\frac{\langle C_\alpha\rangle^{i-2}}{8\Delta Z} \quad (58)$$

where i denotes the ith axial grid position. The resultant matrix at each time step had a lower bandwidth of five and an upper bandwidth of three.

Results and Discussion

The low-pressure experiments identified two vapors, ethanol and 1-propanol, having desirable k and D_β values. Each vapor was used in the high-pressure experiments to examine dispersion. In the following discussion, the evaluation of k and D_β is described first. The values obtained are then used to show that dispersion predicted by the two-equation model of Zanotti and Carbonell is in good agreement with the data from the high-pressure experiments.

Partitioning constant

The values obtained for k are shown in Table 1. Furthermore, as mentioned above, for selected experimental conditions, the total amount of absorbing vapor injected was varied by an order of magnitude, and the same absolute first moments for the vapor concentration at $z=L$ were obtained, which indicated that the value of k was a constant and independent of the vapor concentration used.

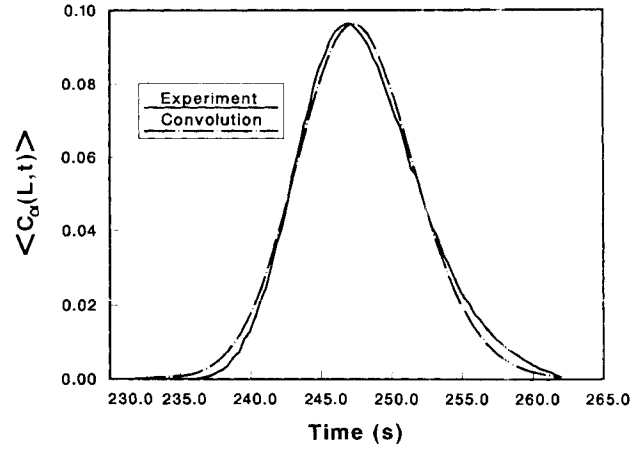

Figure 8. Experimental data vs. convolution solution (Eq. 18) for ethanol at low pressure: $\langle\langle v_\alpha\rangle\rangle = 0.41$ m/s.

β-phase molecular diffusion coefficient

It was shown previously that in the experiments described above, the difference between the area-average concentration $\langle C_\alpha\rangle$ and the flow-average concentration $\overline{C_\alpha}=\overline{c_\alpha}/c^*$ was small. Therefore, when comparing experimental and calculated data, the difference between $\langle C_\alpha\rangle$ and $\overline{C_\alpha}$ was neglected, and all solute concentrations were considered values of $\langle C_\alpha\rangle$. Values of $\langle C_\alpha(L,t)\rangle$ from the low-pressure experiments (average column pressure of 97 kPa) with ethanol and 1-propanol are shown in Figures 7 and 9, respectively. The data for the argon "blanks" corresponding to the same experimental conditions and the analytical values for $\langle C_\alpha(L,t)\rangle$ obtained using the optimized values for D_β and the convolution solution given by Eq. 18 are also shown. The analytical values are essentially superimposed on the experimental data. In Figures 8 and 10, the comparison between the experimental data and the values from the convolution solution with the optimum value of D_β is shown in more detail. The experimental and calculated values for the difference between $\mu_{2\alpha}(L)$ and $\mu_{2\alpha}(0)$ are shown in Table 2, which also shows the analytical values from Eq. 29. For the ethanol data in Figure 8, the difference between $\mu_{2\alpha}(L)$ and $\mu_{2\alpha}(0)$ for the experimental data is about 4% greater than

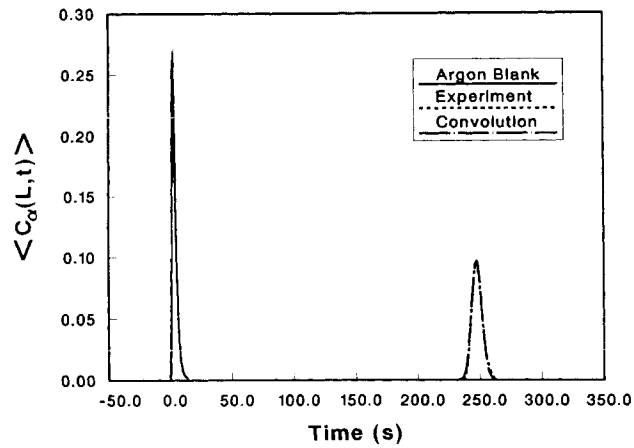

Figure 7. Argon blank and experimental data vs. convolution solution (Eq. 18) for ethanol at low pressure: $\langle\langle v_\alpha\rangle\rangle = 0.41$ m/s.

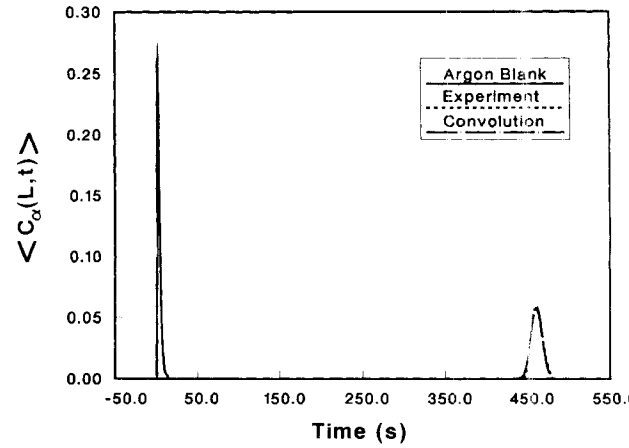

Figure 9. Argon blank and experimental data vs. convolution solution (Eq. 18) for 1-propanol at low pressure: $\langle\langle v_\alpha\rangle\rangle = 0.42$ m/s.

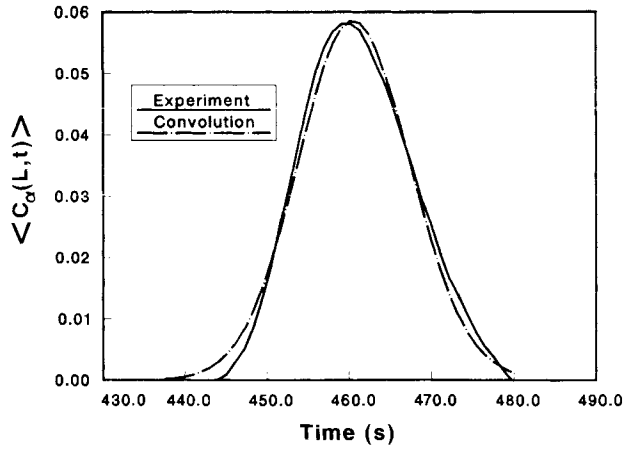

Figure 10. Experimental data vs. convolution solution (Eq. 18) for 1-propanol at low pressure: $\langle\langle v_\alpha\rangle\rangle = 0.42$ m/s.

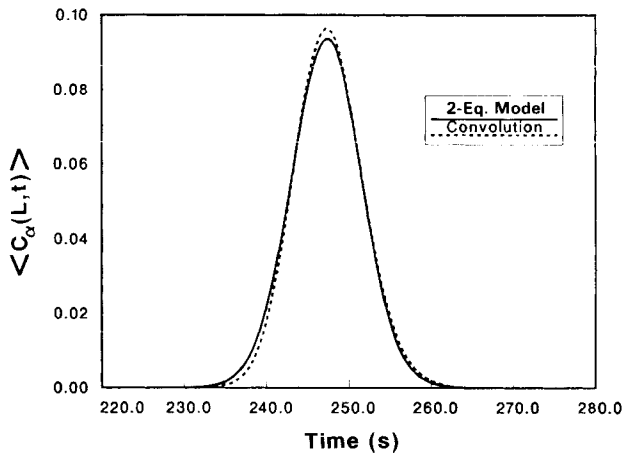

Figure 11. Two-equation model vs. convolution solution (Eq. 18) for ethanol at low pressure.

the difference for the convolution solution given by Eq. 18. For the 1-propanol data in Figure 10, the difference is about 9% less. The values obtained for D_β and the corresponding gas velocities $\langle\langle v_\alpha\rangle\rangle$ are shown in Table 1.

From Eqs. 28 and 29, it can be seen that the analytical second central moment for the two-equation model under conditions of negligible dispersion is the same as that for the film diffusion model, which implies that both models would predict similar values for $\langle C_\alpha(L,t)\rangle$. Figure 11 shows a comparison of results predicted by the two-equation model and the film diffusion model (convolution solution given by Eq. 18) using the parameter values corresponding to the ethanol data shown in Figure 8. As anticipated, the predicted results are similar. The small difference is due probably to a small amount of dispersion neglected in the film diffusion model, or perhaps due to small numerical errors in solving the two-equation model.

Enhanced dispersion: high-pressure results

The film diffusion model underpredicts the dispersion in experimental values of $\langle C_\alpha(L,t)\rangle$ from the high-pressure experiments. A comparison between experimental data for ethanol ($\langle\langle v_\alpha\rangle\rangle = 0.22$ m/s), at an average column pressure of 453 kPa (66 psia), and convolution solution given by Eq. 18 is shown in Figure 12. The difference between the experimental and calculated results is significantly greater than that shown in Figure 11 for the low-pressure experiments. The greater difference in the high-pressure experiments is due primarily to hydrodynamic dispersion, which was illustrated previously in Figures 3 and 4. For the system used in the high-pressure experiments, the difference between $\mu_{2\alpha}(L)$ and $\mu_{2\alpha}(0)$ predicted by the two-equation model is about 15 to 23% greater than that predicted by the film diffusion model. This additional dispersion provided a measurable effect by which the two-equation model of Zanotti and Carbonell could be evaluated.

A comparison of the convolution solution Eq. 18, the numerical solution of the two-equation model, and the experimental data for ethanol, $\langle\langle v_\alpha\rangle\rangle = 0.22$ m/s, is shown in Figure 13. The average column pressure was 453 kPa (66 psia), and the corresponding value of D_α was 9.3×10^{-6} m^2/s. In this case, the difference, shown in Table 3, between $\mu_{2\alpha}(L)$ and $\mu_{2\alpha}(0)$ predicted for only film diffusion (Eq. 29) is 26.54 s^2. The difference predicted by the two-equation model (Eq. 28) is 30.60 s^2, which is about 15% greater than the difference for only film diffusion, and reflects the additional dispersion resulting from molecular diffusion and hydrodynamic effects. Table 4 shows that hydrodynamic effects account for about 84% (3.43/4.06 = 0.84) of the additional dispersion, which is very accurately predicted by the two-equation model, as shown in Figure 13 and further illustrated in Table 3, which shows the good agreement between the values of the difference $\mu_{2\alpha}(L)$ minus $\mu_{2\alpha}(0)$ obtained from the experimental data, numerical solution of the two-equation model, and the moment expression given by Eq. 28.

Table 2. Comparison of Second Central Moments from Experimental Data and Film Diffusion Model: Low-Pressure Experiments

			$\mu_{2\alpha}(L)-\mu_{2\alpha}(0)$ (s^2)		
Vapor	$\langle\langle v_\alpha\rangle\rangle$ (m/s)	$\mu_{2\alpha}(0)$ (s^2)	Exp.	Conv. (Eq. 18)	Anal. (Eq. 29)
Ethanol	0.413	3.86	14.01	13.48	13.95
1-Propanol	0.419	4.91	36.56	40.22	41.87

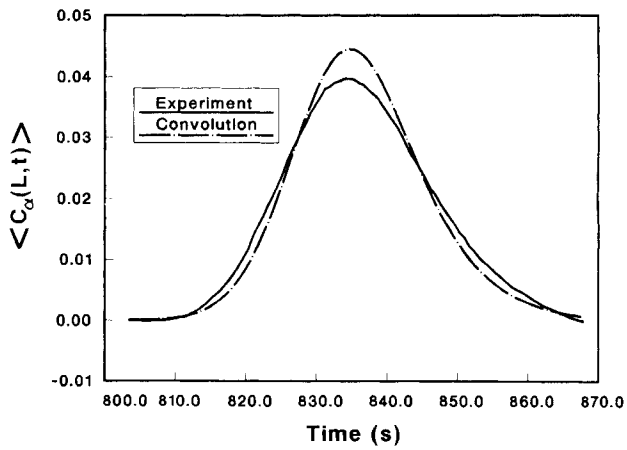

Figure 12. Experimental data vs. convolution solution (Eq. 18) for ethanol at high pressure: $\langle\langle v_\alpha\rangle\rangle = 0.22$ m/s.

Table 3. Comparison of Second Central Moments from Experimental Data, Two-Equation Model, and Film Diffusion Model: High-Pressure Experiments

			$\mu_{2\alpha}(L)-\mu_{2\alpha}(0)$ (s^2)			
				Two-Equation Model		F. D. Model
Vapor	$\langle\langle v_\alpha\rangle\rangle$ (m/s)	$\mu_{2\alpha}(0)$ (s^2)	Exp.	Numer.	Anal. (Eq. 28)	Anal. (Eq. 29)
Ethanol	0.217	9.92	32.63	30.91	30.60	26 54
Ethanol	0.127	44.89	54.98	54.67	54.36	45 35
1-Propanol	0.211	10.30	101.99	101.43	102.14	83 15

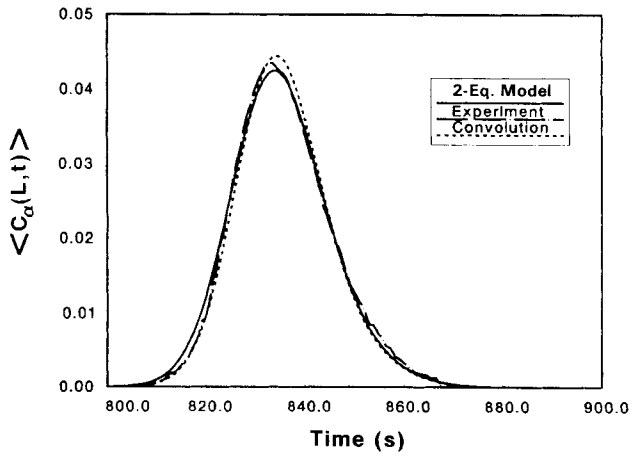

Figure 13. Experimental data vs. two-equation model vs. convolution solution (Eq. 18) for ethanol at high pressure: $\langle\langle v_\alpha\rangle\rangle = 0.22$ m/s.

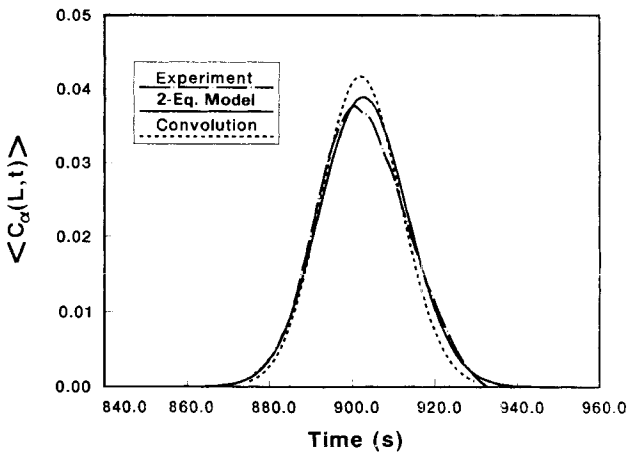

Figure 14. Experimental data vs. two-equation model vs. convolution solution (Eq. 18) for ethanol at high pressure: $\langle\langle v_\alpha\rangle\rangle = 0.13$ m/s.

A second comparison between the two-equation model and experimental data for ethanol is shown in Figure 14 for an average gas velocity $\langle\langle v_\alpha\rangle\rangle$ of 0.13 m/s. The average column pressure was again 453 kPa (66 psia). In this case, the difference between $\mu_{s\alpha}(L)$ and $\mu_{2\alpha}(0)$ (see Table 3) predicted by the two-equation model is about 20% greater than the difference predicted for only film diffusion. The additional dispersion (about 66% due to hydrodynamic effects) is predicted reasonably well by the two-equation model. Table 3 shows the very close agreement between values of the difference $\mu_{2\alpha}(L)$ minus $\mu_{2\alpha}(0)$ obtained from the experimental data, two-equation model, and Eq. 28.

Data for 1-propanol are shown in Figure 15. The value of $\langle\langle v_\alpha\rangle\rangle$ was 0.21 m/s; the average column pressure was 447 kPa (65 psia), and the corresponding value of D_α was 8.4×10^{-6} m^2/s. In this case, the difference between $\mu_{2\alpha}(L)$ and $\mu_{2\alpha}(0)$ (see Table 3) predicted by the two-equation model is about 23% greater than that predicted for only film diffusion. Again, the additional dispersion (about 89% due to hydrodynamic effects) is well predicted by the two-equation model. Furthermore, Table 3 shows excellent agreement between values of the difference $\mu_{2\alpha}(L)$ minus $\mu_{2\alpha}(0)$ obtained from the experimental data, numerical solution of the two-equation model, and Eq. 28.

The agreement between the theory and the experiment shown in Table 3 and Figures 13–15 is summarized in Figure 16, where the ratio μ_2(total)/μ_2(film) calculated from Eqs. 29, 30 and 32 is shown as a function of $\langle\langle v_\alpha\rangle\rangle$. The value of μ_2(film) is the difference between $\mu_{2\alpha}(L)$ and $\mu_{2\alpha}(0)$ from Eq. 29, and μ_2(total) the difference from Eqs. 30 and 32. Values for L, film thickness (r_1-r_0), and r_0 are again 30 m, 1.2×10^{-5} m, and 2.65×10^{-4} m, respectively. The solid line in Figure 16 represents ethanol ($D_\alpha=9.3\times10^{-6}$ m^2/s, $D_\beta=1.2\times10^{-11}$ m^2/s, $k=2.4$), and the dotted line 1-propanol ($D_\alpha=8.4\times10^{-6}$ m^2/s, $D_\beta=8.7\times10^{-12}$ m^2/s, $k=5.3$). The corresponding ratios obtained using the experimentally determined values of the difference $\mu_{2\alpha}(L)$ minus $\mu_{2\alpha}(0)$ for the value of μ_2(total), rather than the value from Eqs. 30 and 32, are shown (by the symbols) and agree well with the theoretical curves. For comparison, the analogous values of μ_2(total)/μ_2(film) calculated from Eqs. 29, 30 and 31

Table 4. Film Diffusion, Molecular Diffusion, and Hydrodynamic Contributions to Dispersion for the Experimental Conditions Corresponding to Figures 13, 14, and 15

	Film Diffusion	Molecular Diffusion	Hydrodynamic Dispersion	
	$\frac{Lk}{\langle\langle v_\alpha\rangle\rangle}\frac{2(r_1-r_0)^2}{3D_\beta}$	$\frac{2L(1+k)^2D_\alpha}{\langle\langle v_\alpha\rangle\rangle^3}$	$\frac{2L}{\langle\langle v_\alpha\rangle\rangle}\frac{r_0^2(1+6k+11k^2)}{48D_\alpha}$	
Figure	(s^2)	(s^2)	(s^2)	$\mu_{2\alpha}(L)-\mu_{2\alpha}(0)$ (s^2)
13	26.54	0.63	3.43	30.60
14	45.35	3.15	5.86	54.36
15	83.15	2.13	16.86	102.14

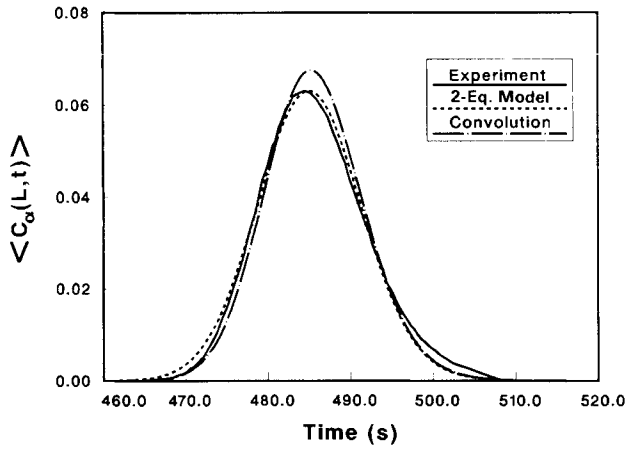

Figure 15. Experimental data vs. two-equation model vs. convolution solution (Eq. 18) for 1-propanol at high pressure: $\langle\langle v_\alpha\rangle\rangle = 0.21$ m/s.

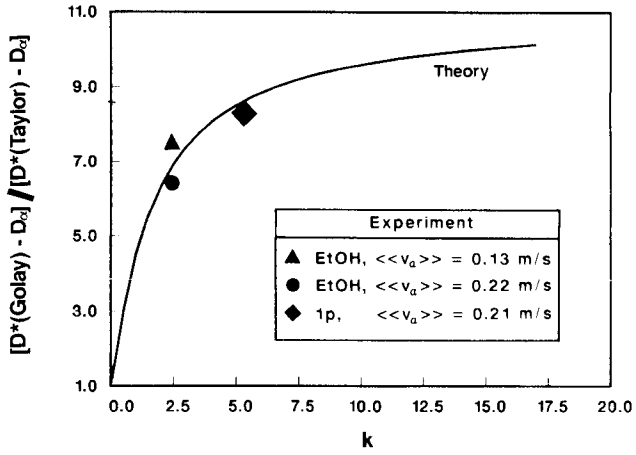

Figure 17. Theory vs. experiment: ratio $[D^*(\text{Golay}) - D_\alpha]/[D^*(\text{Taylor}) - D_\alpha]$ as a function of k.

are also shown and illustrate the relative error incurred when only the Taylor dispersion coefficient (Eq. 31) is used.

In general, the results presented above show that the two-equation model accurately describes both hydrodynamic and film diffusion effects. Furthermore, Golay's expression for the dispersion coefficient is substantiated by the experimental data. This is illustrated in Figure 17, where the ratio

$$\frac{D^*(\text{Golay}) - D_\alpha}{D^*(\text{Taylor}) - D_\alpha} = \frac{1 + 6k + 11k^2}{(1+k)^2} \tag{59}$$

from Eqs. 31 and 32 is shown as a function of k. The corresponding ratios obtained using the experimental data for $\mu_{2\mu}(L)$ and $\mu_{2\alpha}(0)$ in Eq. 30 to determine D^*(Golay) and using Eq. 31 to calculate D^*(Taylor) are also shown (by the symbols) in Figure 17. The average difference between experimental and theoretical values is about 10% (or less) of the theoretical value.

Summary and Conclusions

Experiments were performed to study the enhanced dispersion that results from solute exchange between phases. Ethanol or 1-propanol vapors were injected into an inert carrier gas helium flowing through a long capillary column. The inside wall of the column was coated with a thin vapor-absorbing layer of polyethylene glycol 20M. The molecular diffusion coefficients for ethanol and 1-propanol in the film were determined from independent experiments to accurately determine the coupling of film diffusion and hydrodynamic effects.

The results from the dispersion experiments showed that the two-equation model of Zanotti and Carbonell (1984) accurately describes both film diffusion and hydrodynamic effects. Furthermore, the experimentally observed dispersion that resulted from solute exchange between phases was in quantitative agreement with predictions from the two-equation model and Golay's (1958) earlier analyses, which predicted dispersion coefficients that could be an order-of-magnitude greater than the usual Taylor term.

An extension of the two-equation model to the case of packed beds should be investigated. The enhanced dispersion due to solute exchange between phases or, more generally, due to a mass flux of a solute across a phase boundary could be very pronounced in packed beds with larger-sized particles.

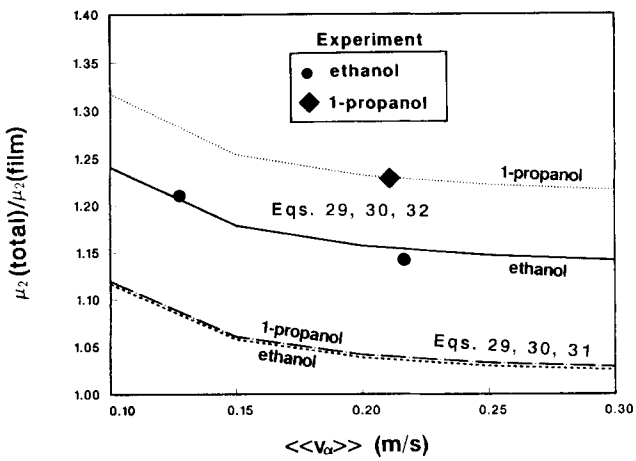

Figure 16. Theory vs. experiment: ratio μ_2(total)/μ_2(film) as a function of $\langle\langle v_\alpha\rangle\rangle$.

Acknowledgment

The authors would like to thank M. R. Baer and J. A. Schutt for invaluable advice on the numerical techniques used. The authors would also like to thank F. D. Chavez for his considerable assistance with the experiments and equipment. This work was performed at Sandia National Laboratories supported by the U. S. Department of Energy under contract no. DE-AC04-76DP00789.

Notation

b = characteristic dimension for an arbitrary tube cross-section, m
$\overline{C_\alpha} = \overline{c_\alpha}/c^*$
$\langle C_\alpha\rangle$ = normalized area-averaged α-phase solute concentration, $\langle c_\alpha\rangle/c^*$
C_β = normalized value of c_β, c_β/c^*K_e
$\langle C_\beta\rangle$ = normalized area-averaged β-phase solute concentration, $\langle c_\beta\rangle/c^*K_e$
$\tilde{c}_\alpha$ = concentration fluctuation defined by Eq. 38, mol/m^3
c_α = local α-phase solute concentration, mol/m^3
$\overline{c_\alpha}$ = flow-averaged α-phase solute concentration defined by Eq. 43, mol/m^3
c_β = local β-phase solute concentration, mol/m^3
c^* = reference solute concentration, $(1/t^*)\int_0^\infty \langle c_\alpha(L,t)\rangle dt$, mol/m^3

$\langle c_\alpha \rangle$ = area average of c_α, $(2/r_0^2)\int_0^{r_0} r c_\alpha dr$, mol/m^3
$\langle c_\beta \rangle$ = area average of c_β, $[2/(r_1^2 - r_0^2)]\int_{r_0}^{r_1} r c_\beta dr$, mol/m^3
D_α = molecular diffusion coefficient for α-phase solute, m^2/s
D_β = molecular diffusion coefficient for β-phase solute, m^2/s
D_e = effective diffusion coefficient, D_β/g, m^2/s
D^* = effective dispersion coefficient defined by Eq. 31 for Taylor dispersion, and by Eq. 32 for Golay dispersion, m^2/s
d_c = coil diameter, m
$F(t)$ = normalized inlet solute concentration
g = dimensionless parameter defined by Eq. 54
I = impulse response defined by Eq. 19, s^{-1}
I_ϕ = impulse response defined by Eq. 52, s^{-1}
K_e = dimensionless absorption equilibrium distribution coefficient
k = dimensionless solute partitioning constant, $K_e(r_1^2 - r_0^2)/r_0^2$ or $2(r_1 - r_0)K_e/r_0$ for $(r_0 - r_1) << r_0$
L = capillary length, m
l = dimensionless parameter defined by Eq. 55
l_1 = minimum value of l
l_2 = maximum value of l
M = β-phase solute concentration per unit area, defined by Eq. 17, mol/m^2
M_ϕ = β-phase solute concentration per unit area, defined by Eq. 48, mol/m^2
$m_{n\alpha}$ = nth moment of $\langle C_\alpha \rangle$, defined by Eq. 24, s^{n+1}
N_{De} = Dean number, defined by Eq. 36
N_{Re} = Reynolds number, defined by Eq. 34
N_{Sc} = Schmidt number, defined by Eq. 35
r = radial position, m
r_0 = radial position of the interface between α and β phases, m
$r_{0_{max}}$ = maximum value of r_0, m
$r_{0_{min}}$ = minimum value of r_0, m
$\overline{r_0}$ = average value of r_0, defined by Eq. 50, m
r_1 = inner radius of capillary tube, m
t = time, s
t^* = unit time, s
v_α = local velocity of the α-phase, m/s
$\langle v_\alpha \rangle$ = area-averaged velocity of the α-phase, $(2/r_0^2)\int_0^{r_0} r \langle v_\alpha \rangle dr$, m/s
$\langle\langle v_\alpha \rangle\rangle$ = axially-averaged value of $\langle v_\alpha \rangle$, defined by Eq. 23, m/s
Z = dimensionless axial position, $zD_\alpha/(\langle\langle v_\alpha \rangle\rangle r_0^2)$
z = axial position, m

Greek letters

γ = dimensionless parameter defined by Eq. 10
Δc = parameter defined by Eq. 40, mol/m^3
$\delta(t)$ = unit impulse symbol, s^{-1}
ϵ = film thickness fluctuation defined by Eq. 49, m
λ = dimensionless curvature ratio, defined by Eq. 37
μ = carrier gas viscosity, g/ms
$\mu'_{n\alpha}$ = absolute nth moment of $\langle C_\alpha \rangle$, defined by Eq. 25, s^n
$\mu_{2\alpha}$ = second central moment of $\langle C_\alpha \rangle$ defined by Eq. 26, s^2
ρ = carrier gas density, g/m^3
Φ = dimensionless constant in Eq. 2
ϕ = azimuthal coordinate, rad
ω = dimensionless variable defined by Eq. 20
ω_ϕ = dimensionless variable defined by Eq. 53

Literature Cited

Aris, R., "On the Dispersion of a Solute in a Fluid Flowing Through a Tube," *Proc. Roy. Soc.*, **A235**, 67, London (1956).

Aris, R., "On the Dispersion of a Solute by Diffusion, Convection and Exchange Between Phases," *Proc. Roy. Soc.*, **A252**, 538, London (1959).

Arnold, D., and R. L. Laurence, "Solute Diffusion in Polymers by Capillary Inverse Gas Chromatography," *Inverse Gas Chromatography, ACS Symp. Ser.*, No. 391, D. R. Lloyd, T. C. Ward, and H. P. Schreiber, eds., Washington, DC, 87 (1989).

Bolvari, A. E., T. C. Ward, P. A. Koning, and D. P. Sheehy, "Experimental Techniques for Inverse Gas Chromatography," *Inverse Gas Chromatography, ACS Symp. Ser.*, No. 391, D. R. Lloyd, T. C. Ward, and H. P. Schreiber, eds., Washington, DC, 15 (1989).

Carbonell, R. G., "Flow Nonuniformities in Packed Beds: Effect on Dispersion," *Chem. Eng. Sci.*, **35**, 1347 (1980).

Dean, W. R., "The Stream-Line Motion of Fluid in a Curved Pipe," *Phil. Mag.*, **5**, 673 (Apr., 1928).

Desty, D. H., and A. Goldup, "Coated Capillary Columns—An Investigation of Operating Conditions," *Gas Chromatography*, R. P. W. Scott, ed., Butterworths, London, 162 (1960).

Erickson, K. L., M. S. Y. Chu, and M. D. Siegel, "Approximate Methods to Calculate Radionuclide Discharges for Performance Assessment of HLW Repositories in Fractured Rock," *Waste Management*, Vol. 2, *Proc. Symp. on Waste Management*, Tucson, AZ, 377 (Mar. 2–6, 1986).

Gill, W. N., and R. Sankarasubramanian, "Exact Analysis of Unsteady Convective Diffusion," *Proc. Roy. Soc.*, **A316**, 341, London (1970).

Golay, M. J. E., "Theory of Chromatography in Open and Coated Tubular Columns with Round and Rectangular Cross Sections," *Gas Chromatography*, D. H. Desty, ed., Butterworths, London, 36 (1958).

IMSL Library, Subroutine ZXSSQ (June, 1980).

Kalb, C. E., and J. D. Seader, "Fully Developed Viscous-Flow Heat Transfer in Curved Tubes with Uniform Wall Temperature," *AIChE J.*, **20**, 340 (Mar., 1974).

Khan, M. A., "Nonequilibrium Theory of Capillary Columns and the Effect of Interfacial Resistance on Column Efficiency," *Gas Chromatography*, M. Van Swaay, ed., Butterworths, Washington, DC, 3 (1962).

Leonard, B. P., "A Stable and Accurate Convective Modelling Procedure Based on Quadratic Upstream Interpolation," *Computer Methods in Applied Mechanics and Engineering*, **19**, 59 (1979).

Levenspiel, O., *Chemical Reaction Engineering*, Wiley, New York, 260 (1962).

Nunge, R. J., T. S. Lin, and W. N. Gill, "Laminar Dispersion in Curved Tubes and Channels," *J. Fluid Mech.*, **51**, 363 (1972).

Paine, M. A., R. G. Carbonell, and S. Whitaker, "Dispersion in Pulsed Systems: 1. Heterogeneous Reaction and Reversible Absorption in Capillary Tubes," *Chem. Eng. Sci.*, **38**, 1795 (1983).

Pawlisch, C. A., J. R. Bric, and R. L. Laurence, "Solute Diffusion in Polymers II. Fourier Estimation of Capillary Inverse Gas Chromatography Data," *Macromolecules*, **21**, 1685 (1988).

Pawlisch, C. A., A. Macris, and R. L. Laurence, "Solute Diffusion in Polymers I. The Use of Capillary Inverse Gas Chromatography," *Macromolecules*, **20**, 1564 (1987).

Reid, R. C., J. M. Prausnitz, and T. K. Sherwood, *The Properties of Gases and Liquids*, McGraw-Hill, New York, 548 (1977).

Rose, A., "Distillation Efficiency in 3- and 6-mm Fractionating Columns," *Ind. Eng. Chem.*, **28**, 1210 (1936).

Rosen, J. B., "General Numerical Solution for Solid Diffusion in Fixed Beds," *Ind. Eng. Chem.*, **46**, 1500 (1954).

Rosen, J. B., "Kinetics of a Fixed Bed System for Solid Diffusion into Spherical Particles," *J. Chem. Phys.*, **20**, 387 (1952).

Scott, R. P. W., and G. S. F. Hazeldon, "Some Factors Affecting Column Efficiency and Resolution of Nylon Capillary Columns," *Gas Chromatography*, R. P. W. Scott, ed., Butterworths, London, 144 (1960).

Shampine, L. F., "DEPAC—Design of a User Oriented Package of ODE Solvers," Report SAND79-2374, Sandia National Laboratories, Albuquerque, NM (Sept., 1980).

Taylor, G. I., "Dispersion of Soluble Matter in Solvent Flowing Slowly Through a Tube," *Proc. Roy. Soc.*, **A219**, 186 (1953).

Trivedi, R. N., and K. Vasudeva, "Axial Dispersion in Laminar Flow in Helical Coils," *Chem. Eng. Sci.*, **30**, 317 (1975).

Valocchi, A. J., "Validity of the Local Equilibrium Assumption for Modelling Sorbing Solute Transport through Homogeneous Soils," *Water Res. Res.*, **21**, 808 (1985).

Van Andel, E., H. Kramers, and A. de Voogd, "The Residence Time Distribution of Laminar Flow in Curved Tubes," *Chem. Eng. Sci.*, **19**, 77 (1964).

Westhaver, J. W., "Theory of Open-Tube Distillation Columns," *Ind. Eng. Chem.*, **34**, 126 (1942).

Zanotti, F., and R. G. Carbonell, "Development of Transport Equations for Multiphase Systems: II. Application of One-Dimensional Axi-Symmetric Flows of Two Phases," *Chem. Eng Sci.*, **39**, 279 (1984).

Manuscript received Mar. 15, 1990, and revision received Feb. 7, 1991.